

Article

# A Colorimetric Assay for the Detection of Glucose and H<sub>2</sub>O<sub>2</sub> Based on Cu-Ag/g-C<sub>3</sub>N<sub>4</sub>/ZIF Hybrids with Superior Peroxidase Mimetic Activity

Quan Pan <sup>1,†</sup>, Yuelin Kong <sup>2,†</sup>, Kuan Chen <sup>2</sup>, Mi Mao <sup>2</sup>, Xiaohui Wan <sup>1</sup>, Xiaoyan She <sup>1</sup>, Qingsong Gao <sup>1</sup>, Yu He <sup>2,\*</sup> and Gongwu Song <sup>2</sup>

<sup>1</sup> Hubei Province Fiber Inspection Bureau, Wuhan 430061, China; panquanfq@163.com (Q.P.); yangguangwxh9272@163.com (X.W.); sxy13871171608@163.com (X.S.); gqs0601@163.com (Q.G.)

<sup>2</sup> Hubei Collaborative Innovation Center for Advanced Organic Chemical Materials, Ministry-of-Education Key Laboratory for the Synthesis and Application of Organic Functional Molecules, College of Chemistry and Chemical Engineering, Hubei University, Wuhan 430062, China; kongyue\_lin@163.com (Y.K.); workout\_k@163.com (K.C.); xxhh\_my@163.com (M.M.); songgw@hubu.edu.cn (G.S.)

\* Correspondence: heyu@hubu.edu.cn

† These authors contributed equally to this work.

Received: 8 September 2020; Accepted: 24 September 2020; Published: 27 September 2020



**Abstract:** In this work, we report the synthesis of Cu-Ag bimetallic nanoparticles and g-C<sub>3</sub>N<sub>4</sub> nanosheets decorated on zeolitic imidazolate framework-8 (ZIF-8) to form a Cu-Ag/g-C<sub>3</sub>N<sub>4</sub>/ZIF hybrid. The hybrid was synthesized and characterized by Transmission electron microscopy (TEM), Fourier transformed infrared (FTIR), the X-ray diffraction (XRD) and X-ray photoelectron spectroscopy (XPS). The Cu-Ag/g-C<sub>3</sub>N<sub>4</sub>/ZIF hybrid has intrinsic peroxidaselike catalytic activity towards the oxidation of TMB in the presence of H<sub>2</sub>O<sub>2</sub>. The situ synthesis of Cu-Ag bimetallic nanoparticles on 2D support such as g-C<sub>3</sub>N<sub>4</sub> nanosheets would significantly enhance the peroxidaselike catalytic properties of individual Cu-Ag bimetallic nanoparticles and the g-C<sub>3</sub>N<sub>4</sub> nanosheets. After loading of Cu-Ag bimetallic nanoparticles and g-C<sub>3</sub>N<sub>4</sub> nanosheets on the ZIF-8, the hybrids exhibited superior peroxidaselike catalytic activity and good recyclability. Then, this method was applied for detecting glucose in human serum, owing the significant potential for detection of metabolites with H<sub>2</sub>O<sub>2</sub>-generation reactions.

**Keywords:** Cu-Ag/g-C<sub>3</sub>N<sub>4</sub>/ZIF hybrid; nanozyme; colorimetric detection; H<sub>2</sub>O<sub>2</sub>; glucose

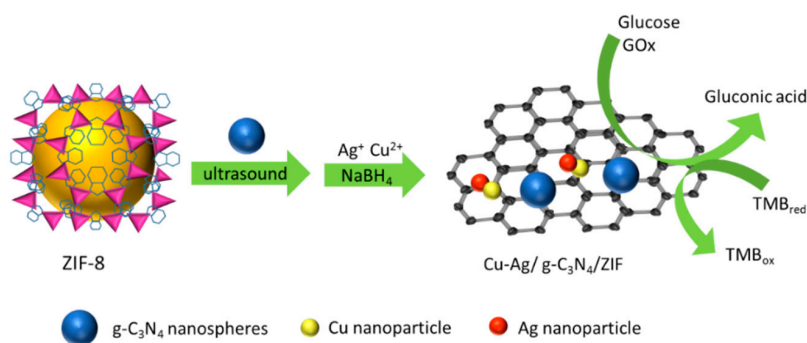
## 1. Introduction

Nanozymes have attracted increasing attention in the past decades in the field of catalysis because of their fantastic advantages, including low cost, facile synthesis, excellent stability and are easy to manipulate in optical sensing [1,2]. After the Fe<sub>3</sub>O<sub>4</sub> nanoparticles was first reported as the peroxidaselike nanoenzyme to catalyze 3,3',5,5'-tetramethylbenzidine (TMB) in the presence of H<sub>2</sub>O<sub>2</sub> to produce a blue color compound 3,3',5,5'-tetramethylbenzidine diimine (TMBDI) [3], different kinds of nanozymes such as carbon based nanomaterials [4], metal nanoparticles [5,6], metal oxides [7,8] and metal oxide nanocomposites [9,10] have been discovered to replace natural enzymes.

Graphitic carbon nitride (g-C<sub>3</sub>N<sub>4</sub>) nanosheets, with similar sheet structure to graphene, have great potential in the catalytic applications of water decomposition, carbon dioxide reduction, organic pollutant degradation and organic synthesis reaction because of their unique band position (2.7 eV) [11–13]. However, the catalytic performance of the g-C<sub>3</sub>N<sub>4</sub> meets some bottlenecks due to its low charge generation efficiency and high photoelectron-hole recombination rate [14]. Therefore, great efforts have been devoted to improve its catalytic activity. Especially, the combination or coupling

of the catalyst with oxides [15,16], metals [17], precious metal nanoparticles [18], sulfide [19,20] and carbon materials [21,22] is an effective method to improve the catalytic activity [23].

Herein, we report on the synthesis of Cu-Ag bimetallic nanoparticles and g-C<sub>3</sub>N<sub>4</sub> nanosheets decorated on zeolitic imidazolate framework-8 (ZIF-8) to form Cu-Ag/g-C<sub>3</sub>N<sub>4</sub>/ZIF nanozyme with intrinsic peroxidaselike catalytic activity towards the oxidation of TMB in the presence of H<sub>2</sub>O<sub>2</sub> (Scheme 1). Cu-Ag bimetallic nanoparticles have been proved to decorate on reduced graphene oxide nanosheets as peroxidase mimic for glucose and ascorbic acid detection [24]. Thus, situ synthesis of Cu-Ag bimetallic nanoparticles on 2D support such as g-C<sub>3</sub>N<sub>4</sub> nanosheets would significantly enhance the peroxidaselike catalytic properties of individual Cu-Ag bimetallic nanoparticles and the g-C<sub>3</sub>N<sub>4</sub> nanosheets. ZIF-8 have been recently investigated as supporters to reduce the consumption rate of metal NPs and restrain their aggregation for its high specific surface area and good thermal and chemical stability [25,26]. After loading of Cu-Ag bimetallic nanoparticles and g-C<sub>3</sub>N<sub>4</sub> nanosheets on the ZIF-8, the hybrids exhibited superior peroxidaselike catalytic activity and good recyclability. Then, a colorimetric method for H<sub>2</sub>O<sub>2</sub> and glucose detection assay was reported based on the color change of TMB with the catalytic reaction of glucose with glucose oxidase (GOx).



**Scheme 1.** Schematic diagram of synthesis of Cu-Ag/g-C<sub>3</sub>N<sub>4</sub>/ZIF hybrid and detection of glucose and H<sub>2</sub>O<sub>2</sub>.

## 2. Results and Discussion

### 2.1. Characterizations of Cu-Ag/g-C<sub>3</sub>N<sub>4</sub>/ZIF Hybrid

TEM and HRTEM image (Figure 1a,b) showed Cu-Ag bimetallic nanoparticles and was g-C<sub>3</sub>N<sub>4</sub> formed on the surface of ZIF-8. The average particle size of Cu-Ag bimetallic nanoparticles was about 5 nm. The alloy nature of Cu-Ag/g-C<sub>3</sub>N<sub>4</sub>/ZIF hybrid is confirmed by the appearance of clear lattice fringes in the HRTEM images. The lattice structures of C<sub>3</sub>N<sub>4</sub> (0.336 nm), Cu NCs (0.207 nm) and Ag NCs (0.23 nm) were observed from Figure 1b, proving that g-C<sub>3</sub>N<sub>4</sub> nanosheets and Cu-Ag bimetallic nanoparticles were loaded onto ZIF-8. The elemental composition and chemical bonding information on the Cu-Ag/g-C<sub>3</sub>N<sub>4</sub>/ZIF hybrid were studied by XPS analysis (Figure 1c,d). The peaks at 933.1 and 952.6 eV were attributed to Cu 2p, belonging to Cu (0), while the peaks at 368.2 and 374.27 eV were attributed to Ag 3d, belonging to Ag (0), indicating that the Cu (0) and Ag (0) were loaded.

The chemical arrangement of the Cu-Ag/g-C<sub>3</sub>N<sub>4</sub>/ZIF hybrid was analyzed by FTIR (Figure 2a,b). In Figure 2a, the absorption band at 1576 cm<sup>-1</sup> was associated with the stretching vibration of CN heterocycle. The peak at 891 cm<sup>-1</sup> could be assigned to the bending vibration of the triazine ring [27]. Compared with bulk-C<sub>3</sub>N<sub>4</sub>, the absorption peak intensity of g-C<sub>3</sub>N<sub>4</sub> in the infrared spectrum was significantly weakened, indicating that part of the CN heterocyclic ring structure was destroyed when bulk-C<sub>3</sub>N<sub>4</sub> was stripped into nanosheets. In Figure 2b, the absorption peaks of 3138 and 2933 cm<sup>-1</sup> were, respectively, the stretching vibration of C-H bond in methyl and imidazole ring, the stretching vibration absorption peaks of C=N bond at 1580 cm<sup>-1</sup> and the stretching vibration absorption peaks of C-N bond at 1145 and 990 cm<sup>-1</sup>, indicating that the framework of the Cu-Ag/g-C<sub>3</sub>N<sub>4</sub>/ZIF hybrid remained intact.

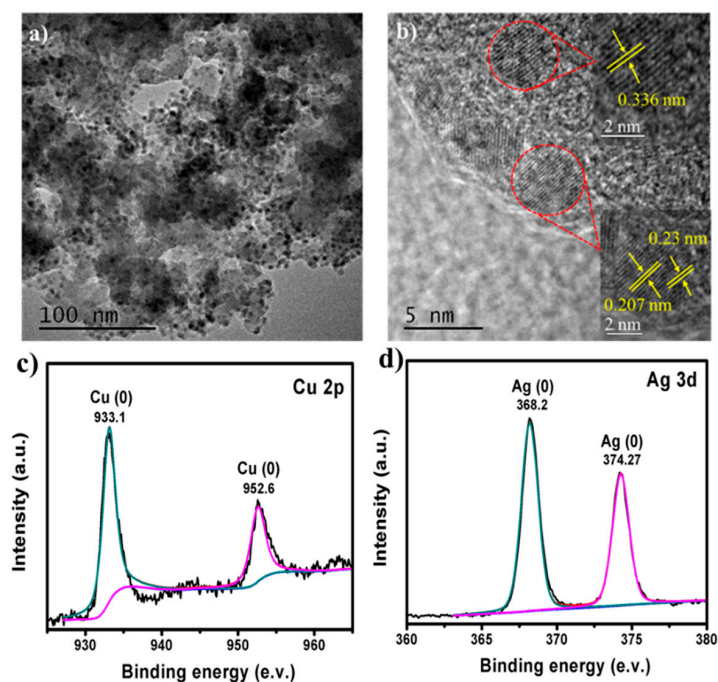


**Figure 1.** (a) TEM images of Cu-Ag/g-C<sub>3</sub>N<sub>4</sub>/ZIF; (b) HRTEM images of Cu-Ag/g-C<sub>3</sub>N<sub>4</sub>/ZIF; (c) XPS spectra of Cu 2p; (d) XPS spectra of Ag3d.

The successful formation of Cu-Ag bimetallic NPs along with the g-C<sub>3</sub>N<sub>4</sub> nanosheet and ZIF-8 is confirmed from XRD analysis (Figure 2c,d). In Figure 2c, compared with the interlayer stacking diffraction peak (002) of bulk-C<sub>3</sub>N<sub>4</sub>, the 002 diffraction peak of the g-C<sub>3</sub>N<sub>4</sub> nanosheet disappeared, indicating that the interlayer stacking of the block was destroyed into a single nanosheet. In Figure 2d, XRD analysis of the Cu-Ag/g-C<sub>3</sub>N<sub>4</sub>/ZIF hybrid showed the same characteristic diffraction peak as ZIF-8, namely (011), (002), (112), (013), (222), (114), (233), (134), (044), (244) and (235). It was proved that the structure of the hybrid was the framework of ZIF-8.

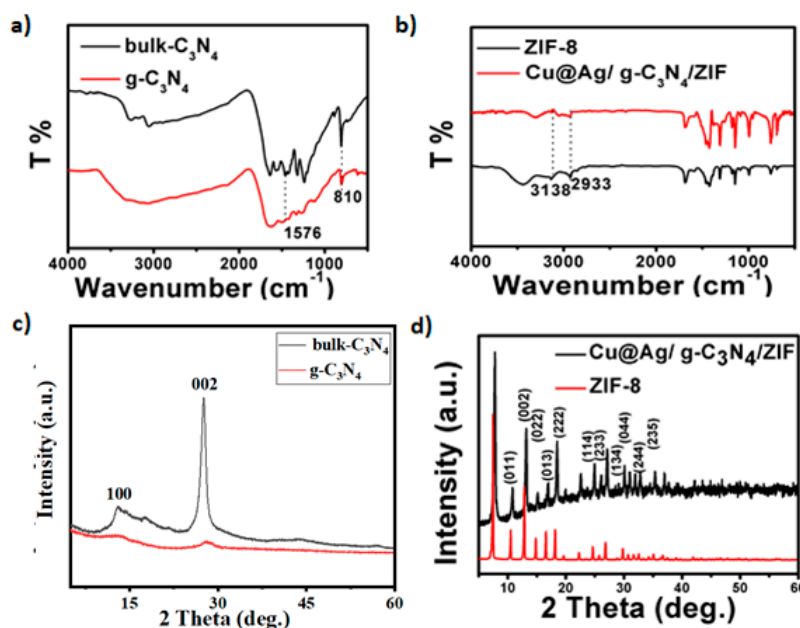


**Figure 2.** (a) FTIR spectra of bulk-C<sub>3</sub>N<sub>4</sub> and g-C<sub>3</sub>N<sub>4</sub>, (b) FT-IR spectra of ZIF-8 and Cu-Ag/g-C<sub>3</sub>N<sub>4</sub>/ZIF, (c) XRD pattern of bulk-C<sub>3</sub>N<sub>4</sub> and g-C<sub>3</sub>N<sub>4</sub>, (d) XRD pattern of ZIF-8 and Cu-Ag/g-C<sub>3</sub>N<sub>4</sub>/ZIF.

## 2.2. Cu-Ag/g-C<sub>3</sub>N<sub>4</sub>/ZIF Hybrid for the Detection of H<sub>2</sub>O<sub>2</sub> and Glucose

The peroxidase-like activity of the Cu-Ag/g-C<sub>3</sub>N<sub>4</sub>/ZIF hybrid was demonstrated by investigating the catalytic oxidation reaction of substrate TMB to a blue 3,3',5,5'-tetramethylbenzidine diimine (TMBDI) in the presence of H<sub>2</sub>O<sub>2</sub>. A comparison of peroxidase-like activity of 25  $\mu$ L H<sub>2</sub>O<sub>2</sub>, 0.3 mg g-C<sub>3</sub>N<sub>4</sub>, 25  $\mu$ L H<sub>2</sub>O<sub>2</sub> and 0.3 mg g-C<sub>3</sub>N<sub>4</sub>, 0.3 mg Cu-Ag/ZIF, 25  $\mu$ L H<sub>2</sub>O<sub>2</sub> and 0.3 mg Cu-Ag/ZIF, 0.3 mg Cu-Ag/g-C<sub>3</sub>N<sub>4</sub>/ZIF; 25  $\mu$ L H<sub>2</sub>O<sub>2</sub> and 0.3 mg Cu-Ag/g-C<sub>3</sub>N<sub>4</sub>/ZIF to TMB is shown in terms of their UV–vis absorption spectra in Figure 3a. The presence of both H<sub>2</sub>O<sub>2</sub> and catalyst is required for the oxidation of TMB to blue TMBDI. The results indicated that the catalytic performance of the Cu-Ag/g-C<sub>3</sub>N<sub>4</sub>/ZIF hybrid was significantly better than that of the g-C<sub>3</sub>N<sub>4</sub> or Cu-Ag/ZIF hybrid. The optimal conditions for peroxidase-like activity of the Cu-Ag/g-C<sub>3</sub>N<sub>4</sub>/ZIF hybrid were determined considering different parameters such as reaction temperature, pH and concentration of TMB (Figures S1–S3). The catalytic activity of the 0.3 mg Cu-Ag/g-C<sub>3</sub>N<sub>4</sub>/ZIF hybrid reached the maximum at 50 °C with the TMB of 500  $\mu$ M and pH of 3.8.

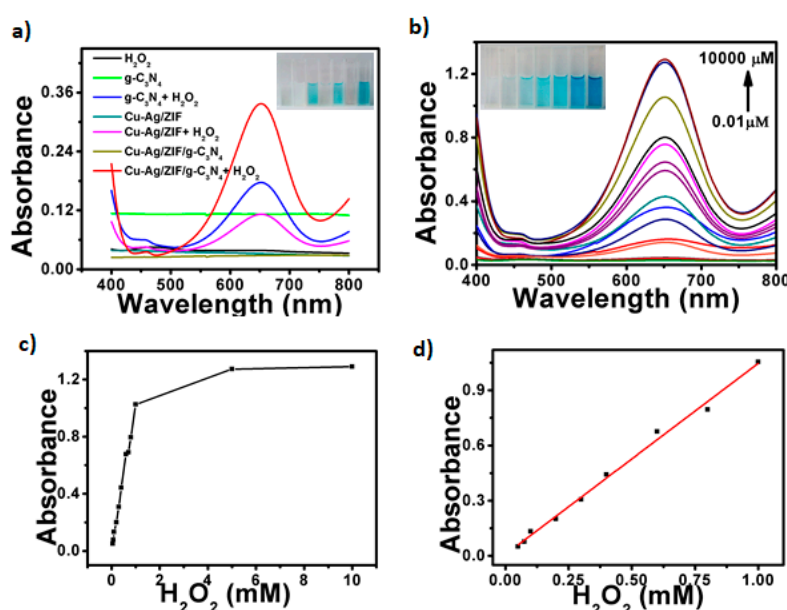


**Figure 3.** (a) Absorption spectra of the reaction of 0.5 mM TMB solution with different catalysts, (b) absorption spectra of TMB solution by Cu-Ag/g-C<sub>3</sub>N<sub>4</sub>/ZIF catalytic reaction with increased H<sub>2</sub>O<sub>2</sub> concentration, (c) detection curves of H<sub>2</sub>O<sub>2</sub> using Cu-Ag/g-C<sub>3</sub>N<sub>4</sub>/ZIF hybrid as the nanoenzyme, (d) the linear calibration plots for H<sub>2</sub>O<sub>2</sub> detection by Cu-Ag/g-C<sub>3</sub>N<sub>4</sub>/ZIF hybrid.

In the presence of both H<sub>2</sub>O<sub>2</sub> and the catalyst, the solution became blue and had significant absorption at 652 nm, indicating that the detection of H<sub>2</sub>O<sub>2</sub> by the Cu-Ag/g-C<sub>3</sub>N<sub>4</sub>/ZIF hybrid was feasible. Figure 3b shows the absorbance at 652 nm against the concentration change of H<sub>2</sub>O<sub>2</sub> from 0 to 10 mM. The linear regression equation is  $A = 1.0389 C + 0.0078$  ( $A$  is the absorbance;  $C$  is also the concentration of glucose in  $\mu$ M) with a linear range from 0.05 to 1 mM, and the limit of detection was calculated to be 2  $\mu$ M (Figure 3c,d).

Because glucose produces gluconic acid and H<sub>2</sub>O<sub>2</sub> in the acidic conditions in the presence of GOx, we designed a colorimetric method for the detection of glucose using a Cu-Ag/g-C<sub>3</sub>N<sub>4</sub>/ZIF hybrid. The result shows that the absorbance at 652 nm enhances significantly with the increasing concentrations of glucose from 0.1 to 2000  $\mu$ M with an limit of detection LOD of 10 nM (Figure 4a,b). The linear regression equation is  $A = 0.0004 C + 0.02886$  with a correlation coefficient of 0.991 ( $A$  is the absorbance;  $C$  is also the concentration of glucose in  $\mu$ M). Furthermore, the color variation is obvious upon visual observation (inset in Figure 4a). For comparison, the detection results of different nanozymes for glucose based on the colorimetric method are listed in Table 1.

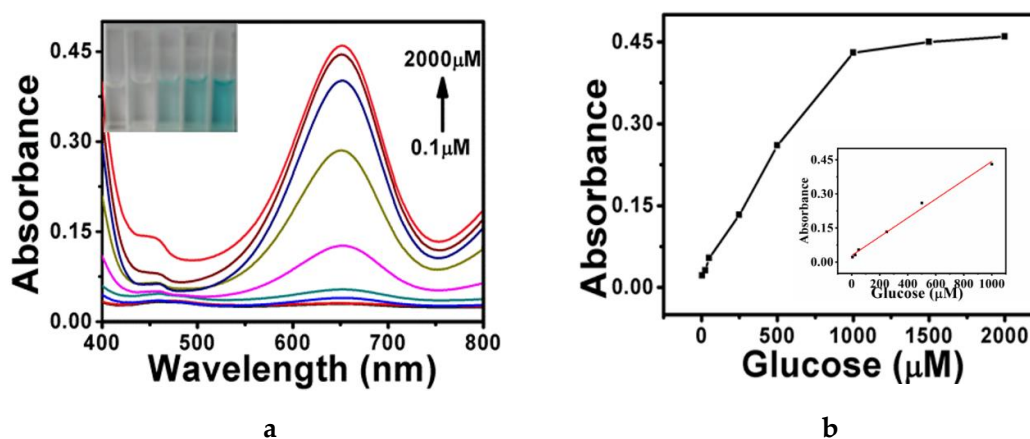


**Figure 4.** (a) Absorption spectra of TMB by Cu-Ag/g-C<sub>3</sub>N<sub>4</sub>/ZIF catalytic reaction with increased glucose concentration, (b) the linear calibration plots for glucose detection by Cu-Ag/g-C<sub>3</sub>N<sub>4</sub>/ZIF hybrid.

**Table 1.** Comparison of the linear range and the limit of glucose detection by various nanozymes.

Nanoenzyme	Lineary Range ( $\mu\text{M}$ )	Detection Limits ( $\mu\text{M}$ )	Ref.
Fe <sub>3</sub> O <sub>4</sub> -porphyrin compositions	5–25	2.21	[24]
Fe <sub>3</sub> O <sub>4</sub> nanoparticles	50–1000	30	[28]
Fe <sub>3</sub> O <sub>4</sub> -GO compositions	1–200	0.74	[3]
Carbon nitride	5–100	1	[29]
Co3O4-rGO compositions	1–100	1	[30]
Cu-Ag/g-C <sub>3</sub> N <sub>4</sub> /ZIF hybrid	0.1–1000	0.01	This work

### 2.3. The Selectivity of Cu-Ag/g-C<sub>3</sub>N<sub>4</sub>/ZIF Hybrid to Glucose Detection

Detection of glucose concentration was an important indicator of clinical diagnosis of glucose. We measured the absorbance response of three glucose analogues, (lactose, fructose and maltose) under the same experimental conditions. From Figure 5, the absorbance of the three glucose analogues at 652 nm was not significantly increased even at a high concentration of 5 mM, while the absorbance of glucose was significantly increased at a concentration of 0.5 mM. The experimental results showed that the Cu-Ag/g-C<sub>3</sub>N<sub>4</sub>/ZIF hybrid had better selectivity to glucose, although all the analogues have similar electron lone pairs and molecular sizes as glucose.

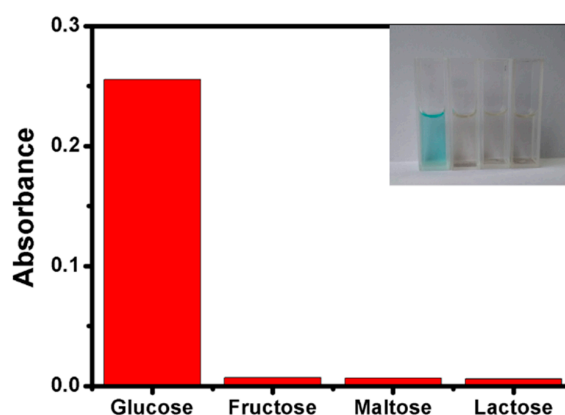


**Figure 5.** Selectivity study of TMB oxidation in the presence of different glucose analogues.

### 2.4. Colorimetric Detection of Glucose in Real Serum Samples

We extended our investigation towards the colorimetric detection of glucose by the Cu-Ag/g-C<sub>3</sub>N<sub>4</sub>/ZIF hybrid as the catalyst in the real serum samples of human volunteers by detecting the

recoveries after adding a given amount of glucose. The performance of the Cu-Ag/g-C<sub>3</sub>N<sub>4</sub>/ZIF hybrid was comparable to that of a commercial glucometer (Table 2). The recovery was between 101.0% and 105.0%. These results suggest that this method is capable of glucose detection in human serum.

**Table 2.** Results of glucose detection in human serum samples.

Sample	Glucometer Method (mM)	Proposed Method (mM)	Added (mM)	Total Found (mM)	Recovery (%)
1	4.87	4.90	3.00	7.93	101.0%
2	5.42	5.38	3.00	8.46	102.7%
3	5.97	6.02	3.00	9.17	105.0%

### 3. Experimental

#### 3.1. Materials and Apparatus

All chemicals were at least analytical grade. Ultrapure water was used throughout the experiments. All solutions were freshly prepared before use. Zinc nitrate tetrahydrate (Zn(NO<sub>3</sub>)<sub>2</sub>·4H<sub>2</sub>O), copper nitrate trihydrate (Cu(NO<sub>3</sub>)<sub>2</sub>·3H<sub>2</sub>O), sodium borohydride (NaBH<sub>4</sub>), methanol (CH<sub>3</sub>OH), N-N-dimethylformamide (DMF), glucose, sulfuric acid (H<sub>2</sub>SO<sub>4</sub>) and hydrogen dioxide (H<sub>2</sub>O<sub>2</sub>) were purchased from Sinopharm Chemical Reagent Co., Ltd. (Shanghai, China). 2-methylimidazole (MeIm) and silver nitrate (AgNO<sub>3</sub>) were purchased from Aladdin Reagent Co., Ltd. (Shanghai, China). Melamine was purchased from McLean Co., Ltd. (Shanghai, China).

The Transmission electron microscopy (TEM) and High Resolution Transmission Electron Microscopy (HRTEM) images of the Cu-Ag/g-C<sub>3</sub>N<sub>4</sub>/ZIF hybrid were examined by FEI High Resolution Transmission Electron Microscopy (Thermo Fisher Scientific, Waltham, MA, USA). Scanning electron microscopy (SEM) images were prepared using a scanning electron microscope (JEOL JSM6510L, Tokyo, Japan). Fourier Transform Infra-Red (FTIR) spectra were taken with a spectrum on a FTIR spectrophotometer (Perkin-Elmer, Waltham, MA, USA). Anode rotating target X-ray diffraction (XRD, Bruker D 8 Advance, Bragg-Brentano, Germany) was carried out to identify crystal structure. The powders deposited on a silicon zero-background sample holder were scanned at a rate of 0.02° (2θ) per second over the range of 5°–60° (2θ). UV-vis absorption spectra were measured at room temperature with a Cary 50 UV-vis spectrophotometer (UV-vis, Shimadzu, Japan) over the range of 200–550 nm. X-ray photoelectron spectroscopy (XPS, ThermoFisher, Hillsboro, OR, USA) measurements were performed using a Thermo Scientific K-Alpha spectrometer.

#### 3.2. One-Step Method to Synthesize Cu-Ag/g-C<sub>3</sub>N<sub>4</sub>/ZIF Hybrid

The bulk g-C<sub>3</sub>N<sub>4</sub> was prepared by direct calcination from melamine: 5 g of melamine was placed in an alumina crucible with a cover and heated from room temperature to 535 °C for 3h, then cooled down naturally. The obtained yellow bulk solid was milled with a quartz mortar and collected. The bulk g-C<sub>3</sub>N<sub>4</sub> was modified via Hummers [31]: Under the condition of ice water bath, 10 g g-C<sub>3</sub>N<sub>4</sub> and 230 mL H<sub>2</sub>SO<sub>4</sub> (98%) were stirred and mixed well. An amount of 30 g KMnO<sub>4</sub> was slowly added and stirred continuously for 30 min. The mixture was transferred to 1.4 L ultrapure water, then 100 mL H<sub>2</sub>O<sub>2</sub> (30%) was added. G-C<sub>3</sub>N<sub>4</sub> was obtained by centrifugation after standing for 24 h. Amounts of 70 mg ZIF-8 and 30 mg g-C<sub>3</sub>N<sub>4</sub> were dispersed in 20 mL methanol solution under ultrasonic condition for 5 min. Amounts of 0.4 mL Cu(NO<sub>3</sub>)<sub>2</sub> (0.0906 g, 0.15 M) and 0.2 mL AgNO<sub>3</sub> (0.0378 g) were added under the protection of N<sub>2</sub>. An amount of 2 mL freshly prepared NaBH<sub>4</sub> solution (0.0743 g, 1 M) was injected during continuously stirring. The Cu-Ag/g-C<sub>3</sub>N<sub>4</sub>/ZIF hybrids were obtained via centrifugation and washed with methanol for three times. The catalyst was dried under vacuum for 5 h, and frozen for preservation.

### 3.3. Cu-Ag/g-C<sub>3</sub>N<sub>4</sub>/ZIF Hybrid for Colorimetric Detection of H<sub>2</sub>O<sub>2</sub> and Glucose

H<sub>2</sub>O<sub>2</sub> detection was performed at 50 °C with pH of 3.5, adjusted with acetate buffer solution. An amount of 0.3 mg catalyst was added to 0.5 mM TMB aqueous solution. The pH was adjusted to 3.8 by acetate buffer solution, making the total volume 2 mL for UV detection. The different concentrations of H<sub>2</sub>O<sub>2</sub> were added into the above solution. After reaction for 20 min in a 50 °C water bath, the absorbance change of the solution at 652 nm was measured, obtaining a linear range of detection of H<sub>2</sub>O<sub>2</sub> by the Cu-Ag/g-C<sub>3</sub>N<sub>4</sub>/ZIF hybrid.

The detection of glucose was performed with the following steps: Firstly, 50 µL 1 mg·mL<sup>-1</sup> glucose oxidase and different concentrations of glucose were incubated at 37 °C with a pH of 7 for 1 h to obtain different concentrations of H<sub>2</sub>O<sub>2</sub> solution. Then, 0.5 mL 2 mM TMB and 0.3 mg catalyst were added into the above solution. Finally, the pH was adjusted to 3.8 by the acetate buffer solution to make a total volume of 2 mL for UV detection. After reaction for 20 min in a 50 °C water bath, the absorbance change of the solution at 652 nm was measured, obtaining a linear range of detection of glucose by the Cu-Ag/g-C<sub>3</sub>N<sub>4</sub>/ZIF hybrid.

## 4. Conclusions

In conclusion, the Cu-Ag/g-C<sub>3</sub>N<sub>4</sub>/ZIF hybrid was synthesized and characterized by Transmission electron microscopy (TEM), Fourier transformed infrared (FTIR), the X-ray diffraction (XRD) and X-ray photoelectron spectroscopy (XPS). The hybrid showed peroxidase-like activity to catalyze the oxidation of TMB to TMBDI in the presence of H<sub>2</sub>O<sub>2</sub>. A facile colorimetric method for detection of the glucose was established by combining the peroxidase-like catalytic activity of the Cu-Ag/g-C<sub>3</sub>N<sub>4</sub>/ZIF hybrid with glucose oxidase. This method was applied for detecting glucose in human serum, owing to the significant potential for the detection of metabolites with H<sub>2</sub>O<sub>2</sub>-generation reactions.

**Supplementary Materials:** Figure S1: Effects of different temperatures on catalytic activity of Cu-Ag/g-C<sub>3</sub>N<sub>4</sub>/ZIF, Figure S2: Effects of different pH on catalytic activity of Cu-Ag/g-C<sub>3</sub>N<sub>4</sub>/ZIF, Figure S3: Effects of different concentration of TMB on catalytic activity of Cu-Ag/g-C<sub>3</sub>N<sub>4</sub>/ZIF.

**Author Contributions:** Data curation X.S.; Funding acquisition, Y.H.; Investigation K.C. and Q.G.; Methodology G.S.; Resources X.W.; Software M.M.; Writing-original draft Q.P. and Y.K., Q.P. and Y.K. contributed equally to this manuscript. All authors have read and agreed to the published version of the manuscript.

**Funding:** This research was funded by National Natural Science Foundation of China grant number 21707030.

**Acknowledgments:** This work was financially supported by the National Natural Science Foundation of China (21707030) and Wuhan Youth Science and technology plan (2016070204010133).

**Conflicts of Interest:** The authors declare no conflict of interest.

## References

1. Darabdhara, G.; Bordoloi, J.; Manna, P.; Das, M.R. Biocompatible bimetallic Au-Ni doped graphitic carbon nitride sheets: A novel peroxidase-mimicking artificial enzyme for rapid and highly sensitive colorimetric detection of glucose. *Sens. Actuators B Chem.* **2019**, *285*, 277–290. [[CrossRef](#)]
2. Wu, N.; Wang, Y.T.; Wang, X.Y.; Guo, F.N.; Wen, H.; Yang, T.; Wang, J.H. Enhanced peroxidase-like activity of AuNPs loaded graphitic carbon nitride nanosheets for colorimetric biosensing. *Anal. Chim. Acta* **2019**, *1091*, 69–75. [[CrossRef](#)] [[PubMed](#)]
3. Gao, L.; Zhuang, J.; Nie, L.; Zhang, J.; Zhang, Y.; Gu, N.; Wang, T.; Feng, J.; Yang, N.; Perrett, S.; et al. Intrinsic peroxidase-like activity of ferromagnetic nanoparticles. *Nat. Nanotechnol.* **2007**, *2*, 577–583. [[CrossRef](#)] [[PubMed](#)]
4. Sun, H.; Zhou, Y.; Ren, J.; Qu, X. Carbon nanozymes: Enzymatic properties, catalytic mechanism, and applications. *Angew. Chem. Int. Ed.* **2018**, *57*, 9224–9237. [[CrossRef](#)] [[PubMed](#)]
5. Du, Z.; Wei, C. Using G-Rich sequence to enhance the peroxidase-mimicking activity of DNA-Cu/Ag nanoclusters for rapid colorimetric detection of hydrogen peroxide and glucose. *Chem. Select* **2020**, *5*, 5166–5171. [[CrossRef](#)]

6. Mirhosseiniab, M.; Farab, A.S.; Hakimianbc, F.; Haghirsadat, B.F.; Fatemi, S.K.; Dashtestanib, F. Core-shell Au@Co-Fe hybrid nanoparticles as peroxidase mimetic nanozyme for antibacterial application. *Process. Biochem.* **2020**, *95*, 131–138. [[CrossRef](#)]
7. Lian, J.; Liu, P.; Jin, C.; Shi, Z.; Luo, X.; Liu, Q. Perylene diimide-functionalized CeO<sub>2</sub> nanocomposite as a peroxidase mimic for colorimetric determination of hydrogen peroxide and glutathione. *Microchim. Acta* **2019**, *186*, 332. [[CrossRef](#)]
8. Zhang, B.; Huyan, Y.; Wang, J.; Wang, W.; Zhang, Q.; Zhang, H. Synthesis of CeO<sub>2</sub> nanoparticles with different morphologies and their properties as peroxidase mimic. *J. Am. Ceram. Soc.* **2019**, *102*, 2218–2227. [[CrossRef](#)]
9. Yang, W.N.; Li, J.; Yang, J.; Liu, Y.; Xu, Z.P.; Sun, X.F.; Wang, F.D. Biomass-derived hierarchically porous CoFe-LDH/CeO<sub>2</sub> hybrid with peroxidase-like activity for colorimetric sensing of H<sub>2</sub>O<sub>2</sub> and glucose. *J. Alloys Compd.* **2020**, *815*, 152276.
10. Xing, Y.; Si, H.; Sun, D.; Hou, X. Magnetic Fe<sub>3</sub>O<sub>4</sub>@NH<sub>2</sub>-MIL-101(Fe) nanocomposites with peroxidase-like activity for colorimetric detection of glucose. *Microchem. J.* **2020**, *156*, 104929. [[CrossRef](#)]
11. Wang, X.; Maeda, K.; Thomas, A.; Takane, K.; Xin, G.; Carlsson, J.M.; Domen, K.; Antonietti, M. A metal-free polymeric photocatalyst for hydrogen production from water under visible light. *Nat. Mater.* **2009**, *8*, 76–80. [[CrossRef](#)] [[PubMed](#)]
12. Algara-Siller, G.; Severin, N.; Chong, S.Y.; Björkman, T.; Palgrave, R.G.; Laybourn, A.; Antonietti, M.; Khimiyak, Y.Z.; Krasheninnikov, A.V.; Rabe, J.P.; et al. Triazine-based graphitic carbon nitride: A two-dimensional semiconductor. *Angew. Chem.* **2014**, *126*, 7580–7585. [[CrossRef](#)]
13. Cao, S.W.; Low, J.; Yu, J.; Jaroniec, M. Polymeric photocatalysts based on graphitic carbon nitride. *Adv. Mater.* **2015**, *27*, 2150–2176. [[CrossRef](#)]
14. Zhou, D.; Wang, C.; Luo, J.; Yang, M. C<sub>3</sub>N<sub>4</sub> nanosheet-supported Prussian Blue nanoparticles as a peroxidase mimic: Colorimetric enzymatic determination of lactate. *Microchim. Acta* **2019**, *186*, 735. [[CrossRef](#)] [[PubMed](#)]
15. Wang, Y.; Shi, R.; Lin, J.; Zhu, Y. Enhancement of photocurrent and photocatalytic activity of ZnO hybridized with graphite-like C<sub>3</sub>N<sub>4</sub>. *Energy Environ. Sci.* **2011**, *4*, 2922–2929. [[CrossRef](#)]
16. Bai, X.; Wang, L.; Zhu, Y. Visible photocatalytic activity enhancement of ZnWO<sub>4</sub> by graphene hybridization. *Adv. Funct. Mater.* **2012**, *22*, 1518–1524. [[CrossRef](#)]
17. Tonda, S.; Kumar, S.; Shanker, V. Surface plasmon resonance-induced photocatalysis by Au nanoparticles decorated mesoporous g-C<sub>3</sub>N<sub>4</sub> nanosheets under direct sunlight irradiation. *Mater. Res. Bull.* **2016**, *75*, 51–58. [[CrossRef](#)]
18. Fu, Y.; Huang, T.; Jia, B.; Zhu, J.; Wang, X. Reduction of nitrophenols to aminophenols under concerted catalysis by Au/g-C<sub>3</sub>N<sub>4</sub> contact system. *Appl. Catal. B Environ.* **2017**, *202*, 430–437. [[CrossRef](#)]
19. Fu, J.; Chang, B.B.; Tian, Y.L.; Xi, F.N.; Dong, X.P. Novel C<sub>3</sub>N<sub>4</sub>-CdS composite photocatalysts with organic-inorganic heterojunctions: In situ synthesis, exceptional activity, high stability and photocatalytic mechanism. *J. Mater. Chem. A.* **2013**, *1*, 3083–3090. [[CrossRef](#)]
20. Wang, J.; Guo, P.; Guo, Q.S.; Jonsson, P.G.; Zhao, Z. Fabrication of novel g-C<sub>3</sub>N<sub>4</sub>/nanocage ZnS composites with enhanced photocatalytic activities under visible light irradiation. *Cryst. Eng. Comm.* **2014**, *16*, 4485–4492. [[CrossRef](#)]
21. Li, Y.B.; Zhang, H.M.; Liu, P.R.; Wang, D.; Li, Y.; Zhao, H.J. Cross-linked g-C<sub>3</sub>N<sub>4</sub>/rGO nanocomposites with tunable band structure and enhanced visible light photocatalytic activity. *Small* **2013**, *9*, 3336–3344. [[CrossRef](#)]
22. Liu, J.; Liu, Y.; Liu, N.; Han, Y.; Zhang, X.; Huang, H.; Lifshitz, Y.; Lee, S.T.; Zhong, J.; Kang, Z. Metal-free efficient photocatalyst for stable visible water splitting via a two-electron pathway. *Science* **2015**, *347*, 970–974. [[CrossRef](#)] [[PubMed](#)]
23. Xiong, Z.G.; Zhao, X.S. Nitrogen-doped titanate-anatase core-shell nanobelts with exposed {101} anatase facets and enhanced visible light photocatalytic activity. *J. Am. Chem. Soc.* **2012**, *134*, 5754–5757. [[CrossRef](#)]
24. Darabdhara, G.; Sharma, B.; Dasa, M.R.; Boukherrou, R.; Szunerits, S. Cu-Ag bimetallic nanoparticles on reduced graphene oxidenanosheets as peroxidase mimic for glucose and ascorbic acid detection. *Sens. Actuators B Chem.* **2017**, *238*, 842–851. [[CrossRef](#)]
25. Song, X.; Sun, H.; Cao, X.; Wang, Z.; Zhao, D.; Sun, J.; Zhang, H.; Li, X. Hierarchically porous ternary Au/ZnO@ZIF-8 nanocomposite: Spatial in situ Au encapsulation and catalytic activity for the reduction of p-nitrophenol. *RSC Adv.* **2016**, *6*, 112451–112454. [[CrossRef](#)]

26. Yang, L.; Yan, D.; Liu, C. Vertically oriented reduced graphene oxide supported dealloyed palladium–copper nanoparticles for methanol electrooxidation. *J. Power Sources* **2015**, *278*, 725–732. [[CrossRef](#)]
27. Wang, X.; Shen, Y.; Xie, A.; Qiu, L.; Li, S.; Wang, Y. Novel structure CuI/PANI nanocomposites with bifunctions: Superhydrophobicity and photocatalytic activity. *J. Mater. Chem. A* **2011**, *21*, 9641–9646. [[CrossRef](#)]
28. Cash, K.J.; Clark, H.A. Nanosensors and nanomaterials for monitoring glucose in diabetes. *Trends Mol. Med.* **2010**, *16*, 584–593. [[CrossRef](#)]
29. Song, Y.; Qu, K.; Zhao, C.; Ren, J.; Qu, X. Graphene oxide: Intrinsic peroxidase catalytic activity and its application to glucose detection. *Adv. Mater.* **2010**, *22*, 2206–2210. [[CrossRef](#)]
30. Shi, W.; Wang, Q.; Long, Y.; Cheng, Z.; Chen, S.; Zheng, H.; Huang, Y. Carbon nanodots as peroxidase mimetics and their applications to glucose detection. *Chem. Commun.* **2011**, *47*, 6695–6697. [[CrossRef](#)]
31. Giannakoudakis, D.A.; Seredych, M.; Rodríguez-Castellón, E.; Bandosz, T.J. Mesoporous graphitic carbon nitride-based nanospheres as visible-light active chemical warfare agents decontaminant. *ChemNanoMat* **2016**, *2*, 268–272. [[CrossRef](#)]

**Sample Availability:** Samples of the compounds not available from the authors.



© 2020 by the authors. Licensee MDPI, Basel, Switzerland. This article is an open access article distributed under the terms and conditions of the Creative Commons Attribution (CC BY) license (<http://creativecommons.org/licenses/by/4.0/>).